

# Fabrication and Magnetic Characterization of Embedded Permalloy Structures

T. Matsumoto, T. Tezuka, T. Ishibashi, Y. Morishita, A. Koukitu, and K. Sato

Faculty of Technology, Tokyo University of Agriculture and Technology, Koganei, Tokyo 184-8588

Magnetic nanostructures embedded in silicon wafers were successfully fabricated by the damascene technique using electron beam lithography. The magnetic properties of embedded square dots (1  $\mu\text{m}$  in width and 100 nm in height), rectangular dots (300 nm  $\times$  100 nm in area and 100 nm in height), and circular dots (100 nm in diameter and 100 nm in height) were investigated. Magnetic force microscopy (MFM) and vibrating sample magnetometer (VSM) measurements showed that the perpendicular anisotropy increased with the aspect ratio, due to a decrease in the areal size. Fine magnetic structures of the 300 nm  $\times$  100 nm pattern were clearly resolved by using a special MFM with a low-moment tip.

**Key words:** magnetic nanostructures, electron beam lithography, damascene techniques, magnetic force microscopy

## 1. Introduction

Fabrication of magnetic nanostructures is attracting attention because of growing interest in research on patterned magnetic recording media,<sup>1)</sup> as well as nano-magnetic science. For these types of research, establishment of techniques for the fabrication and characterization of magnetic nanostructures is becoming more and more important.

Recent advances in nano-fabrication technologies such as electron beam (EB) lithography and focused ion-beam (FIB) technology have made it possible to fabricate magnetic structures with nanometer to sub-micrometer dimensions, while developments in probe techniques have enabled characterization of such magnetic fine structures.

A number of interesting reports have already been published by various research institutions.<sup>2-5)</sup> Most of these studies utilize lift-off processes or ion beam milling as fabrication technologies, due to their practicality. However, these methods introduce uneven surfaces, which are not suited for use in patterned media. Uneven surfaces have also been known to cause undesirable signals in magnetic force microscope (MFM) imaging. To obtain flat embedded structures of CoPt dot arrays TDK researchers employed damascene techniques using SiO<sub>2</sub> substrates.<sup>6)</sup>

We also adopted a damascene technique to fabricate magnetic dot arrays, but in the present study, we used silicon instead of SiO<sub>2</sub> to embed magnetic materials,

because it facilitates the use of nano-fabrication techniques in semiconductor device fabrication. Pit array structures were fabricated using EB patterning and a dry-etching process well established in semiconductor technology. Magnetic films were deposited on the pit-arrays and magnetic materials outside the pits were removed by using a chemical mechanical polishing (CMP) method to obtain a flat embedded structure. Using the embedded magnetic structures obtained, not only can we obtain good MFM images of magnetic dot arrays avoiding the superposition of topographic images, but we can also easily measure magneto-optical responses by virtue of the flat surface.

As a magnetic material to be embedded, we employed permalloy (Ni<sub>80</sub>Fe<sub>20</sub>) in this work. Since permalloy is known to be a soft material with low magnetic anisotropy, it is suited for studying structure-induced magnetic properties, although we know that this material is not suited for magnetic storage. We believe, however, that the results of the research on nano-fabrication technology conducted here may be applicable to patterned disk technology.

## 2. Experiment

The process flow of the damascene technique with EB lithography for fabrication of permalloy-dot array structures is schematically illustrated in Fig. 1.

As a substrate in which to embed magnetic material, we employed a Si(100) wafer. An EB-resist (ZEP-520 supplied by Nippon Zeon Co., Ltd.), which has an excellent dry-etching resistance, was spin-coated at a rotation speed of 5000 rpm, followed by baking at 160°C for 20 min before EB exposure. The thickness of the resist was about 300 nm.

Arrays of square, rectangular, and circular dots as well as lines were patterned on the resist using an electron-beam pattern generator (JEOL type JBX-5000SH). The patterned resist was developed using a ZED-N50 (n-Amyl acetate) developer. The patterned area was 3 mm  $\times$  3 mm.

Using the patterned resist as a mask, the Si substrate was plasma-etched using CF<sub>4</sub> gas with an RF power of 400 W, in which the etching process proceeded as a chemical reaction between the Si wafer and the F radicals. Since the dry-etching process is isotropic in nature, it often leads to the formation of an undercut below the mask. To prevent this phenomenon and to

keep the etching anisotropic, precise control of the etching time was necessary; however, this limited the depth of the structure. The optimum etching rate was found to be about 0.1  $\mu\text{m}$  per minute. The remaining resist was finally removed in an ultrasonic bath using acetone.

By this method, an array of pits with a depth of less than 150 nm was uniformly formed over an area 3 mm  $\times$  3 mm in size. A permalloy film was deposited by using an EB evaporator. The thickness was monitored during evaporation by a thickness monitor using a quartz crystal oscillator to adjust the evaporation period, thus assuring that the deposited film had the same thickness as the pit depth. The typical deposition rate was 1.0  $\text{\AA}/\text{s}$ .

In order to remove the permalloy film deposited outside the pits and obtain a flat surface, we performed CMP. The polishing was carried out by using a pH-controlled chemical solution that included polishing slurry (Glanzox SP-15, Fujimi Corp.).

The samples were placed on the rotating polishing cloth, to which the slurry was supplied. The polishing rate was adjusted by a combination of mechanical

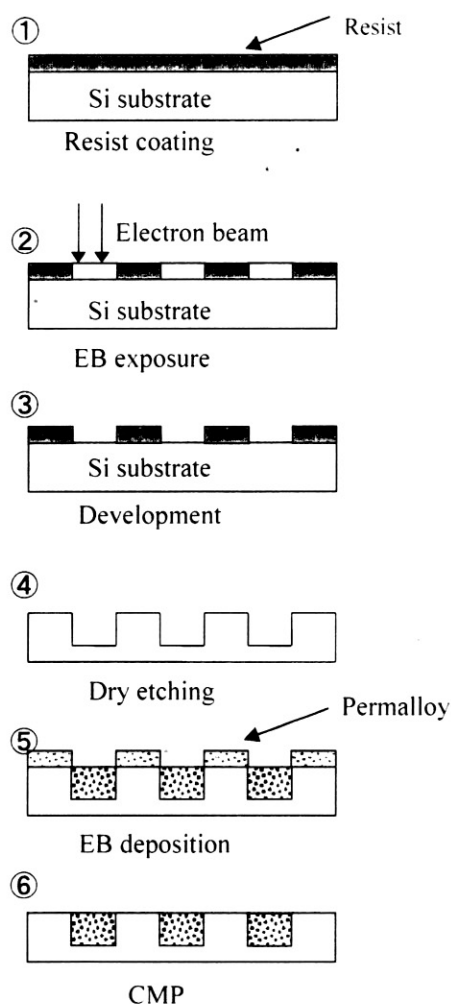


Fig. 1 Fabrication process for a permalloy dot array patterned by the damascene technique.

polishing and etching for chemical reaction.

Three kinds of structures were prepared: 1  $\mu\text{m}$   $\times$  100 nm square dot arrays, 300 nm  $\times$  100 nm rectangular dot arrays and circular dot arrays with a diameter of 100 nm. The depth of these patterns was kept at 100 nm, and separation between dots in these structures was kept at 300 nm in the present study. A line-and-space pattern with a width of 100 nm, a depth of 140 nm, and a repetition period of 1  $\mu\text{m}$  was also prepared as a reference.

### 3. Results and Discussion

#### 3.1 Characterization of the sample configuration

The scanning electron microscope (SEM) images of the fabricated rectangular dots and circular dots after the CMP process (Fig. 2) show that these samples were successfully obtained as designed by EB lithography. The edges of rectangular dots became rounded on account of the spot shape of the electron beam. Thus it is difficult to obtain an exact rectangular shape for 100 nm size.

Figure 3 shows a cross-sectional SEM image of a line-and-space pattern with a line width of 100 nm. We can see that the permalloy is successfully embedded into the silicon, with a depth of about 140 nm. The line-scan profile measured using an atomic force microscope

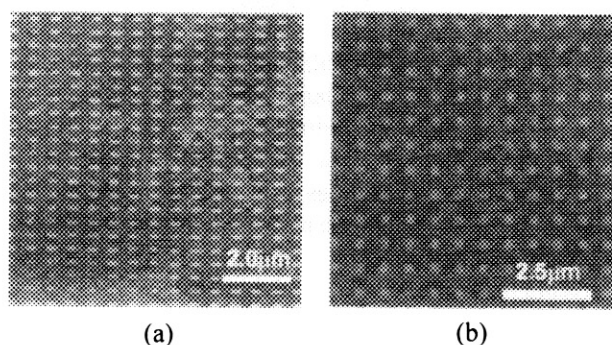


Fig. 2 SEM image of (a) rectangular dot arrays and (b) circular dot arrays.

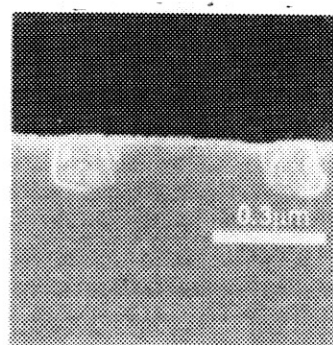


Fig. 3 SEM image of a cross-section of an embedded permalloy structure with a line-and-space pattern.

(AFM) showed that the rms roughness of the sample surface was only about 10 nm. Some of the samples showed unevenness of less than 2 nm. These results indicate that we have established a fabrication technique for embedded permalloy nanostructures with a considerable depth exceeding 100 nm.

### 3.2 Magnetic properties of the square dot arrays

The magnetic properties of these samples were measured by using a vibrating sample magnetometer (VSM) (Toei type VSM-5) and an MFM (Seiko Instruments type SPI-3800N). MFM images were obtained in a tapping/lift mode in order to keep the distance between the sample and the MFM tip constant, and were measured at remanent states in the air.

Thickness of the magnetic CoCr coating on the MFM tip used in the present study was 80 nm. The tip-sample distance was 2–3 nm during the AFM sensing and 80 nm during the MFM measurement.

Figure 4 shows VSM measurement of hysteresis loops in the magnetic structures, consisting of square dots with dimensions of  $1\ \mu\text{m} \times 1\ \mu\text{m} \times 100\ \text{nm}$  and spacing of 300 nm. Figure 5 shows (a) AFM and (b) MFM images of the square dot array.

The hysteresis loops show that  $H_c$  and  $M_r/M_s$  are 60 Oe and 0.2, respectively for in-plane magnetization, and 80 Oe and 0.23, respectively, for perpendicular magnetization. The value of  $H_c$  increased to 10 times that of unpatterned permalloy thin films with a thickness of 100 nm deposited by an EB evaporator under the same conditions, while  $M_r/M_s$  decreased to about 1/4 of that for in-plane magnetic field.

The MFM image shows well-defined closure domain structures in the observed area of  $4\ \mu\text{m} \times 4\ \mu\text{m}$ . Cross-shaped bright images corresponding to a  $90^\circ$ -domain wall were clearly observed. However, they were found to be subject to propeller-like distortion. Similar results were reported by Miltat et al., and were explained in terms of the effect of the stray field from an MFM tip.<sup>7)</sup>

### 3.3 Magnetic properties of rectangular dot arrays

Figures 6 and 7 show hysteresis loops and MFM images, respectively, of patterns consisting of rectangular dots with an area of  $300\ \text{nm} \times 100\ \text{nm}$  and a height of 100 nm. The hysteresis loops show that  $H_c$  and  $M_r/M_s$  are 50 Oe and 0.25, respectively, for magnetization in the plane along the longer axis and 100 Oe and 0.24, respectively for perpendicular magnetization. Notice that perpendicular anisotropy is enhanced in relation to the  $1\ \mu\text{m} \times 1\ \mu\text{m}$  square dots.

MFM images were measured in two different scanning directions: (a) parallel to the longer axis of the rectangle and (b) parallel to the shorter axis, as schematically shown in Fig. 7. Clearly the MFM image

depends on the scanning direction, suggesting that the magnetic field from the MFM tip has a considerable influence on the observed pattern.

This result poses a serious problem for measurement of soft magnetic materials using MFM. In order to solve the problem, MFM images were measured at Seiko Instruments Corp. by using a low-moment tip in vacuum.<sup>8)</sup> The thickness of the magnetic material coated on the tip was as little as 24 nm. AFM and MFM images are shown in Figs. 8(a) and 8(b), respectively. The scanning direction was the same as in Fig. 7(b). Two sets of bright-dark contrast patterns were observed in one dot, consistent with the small remanent magnetization observed in VSM measurements.

The results of VSM and MFM measurements suggest that the rectangular dots with an areal dimension of  $300\ \text{nm} \times 100\ \text{nm}$  and a height of 100 nm have a three-dimensional vortex structures. It should be noted, however, that the MFM image is influenced by the magnetic field from the probe tip, even if a low-moment tip is used. The magnetic structures observed in the MFM images are very complex, which may presumably be attributed to unavoidable roughness produced during the fabrication process. Micro-magnetic simulation of the nano-magnetic structures is necessary for further analysis.

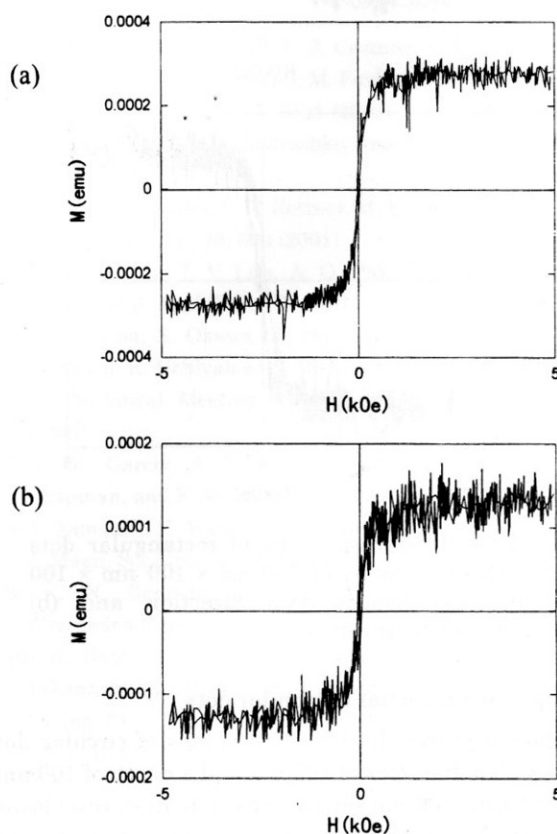


Fig. 4 Hysteresis loops of square dots with dimensions of  $1\ \mu\text{m} \times 1\ \mu\text{m} \times 100\ \text{nm}$  for magnetic fields (a) parallel to and (b) perpendicular to the sample plane.

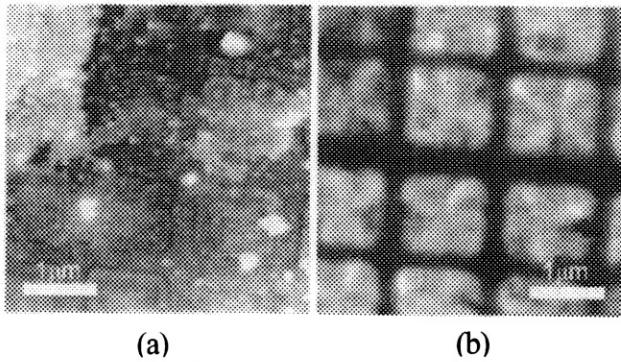


Fig. 5 (a) AFM image and (b) MFM image of square dots.

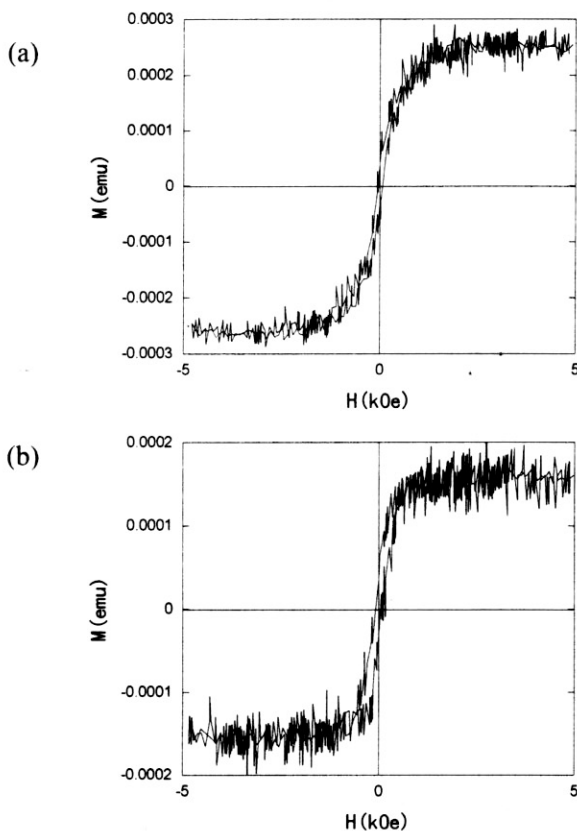


Fig.6 Hysteresis loops of rectangular dots with dimensions of  $300 \text{ nm} \times 100 \text{ nm} \times 100 \text{ nm}$ . (a) Longer axis direction and (b) perpendicular direction

### 3.4 Magnetic properties of circular dots

Figure 9 shows the hysteresis loops of circular dot arrays with a diameter of 100 nm and a depth of 100 nm arranged with 300 nm separations. The hysteresis loops show that  $H_c$  and  $M_r/M_s$  are 80 Oe and 0.3, respectively, for magnetization parallel to the sample surface, and 100 Oe and 0.17, respectively, for magnetization perpendicular to the surface. It can be clearly seen that the circular dots with a diameter of 100 nm and a depth

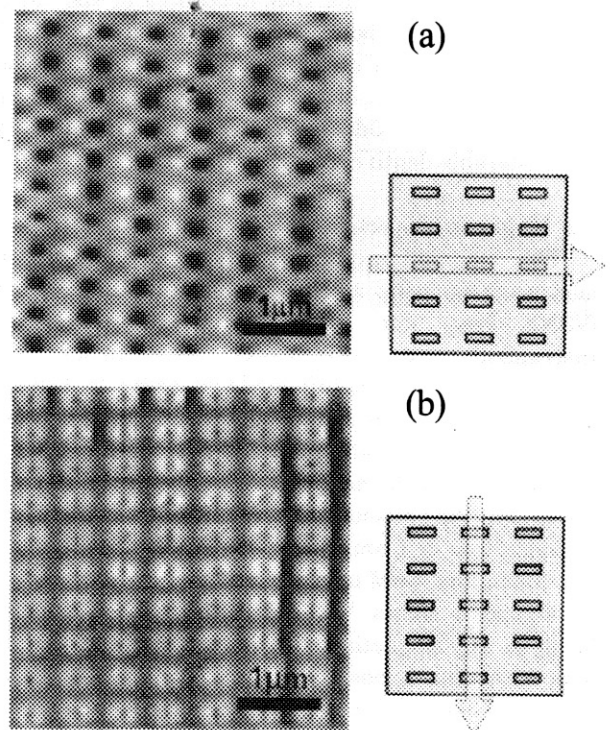


Fig. 7 (a) MFM image scanned along the longer axis of rectangular dots and (b) MFM image scanned along the shorter axis. Arrows in the drawings denote the scanning direction.

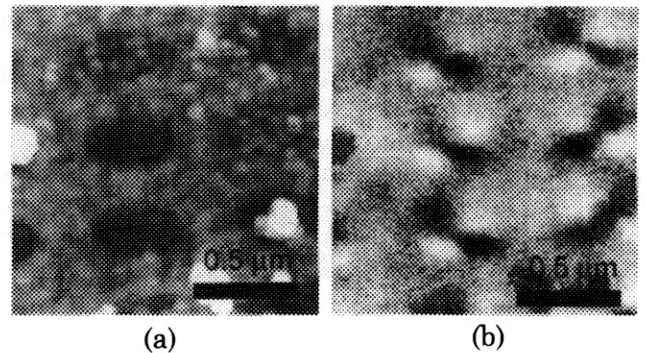
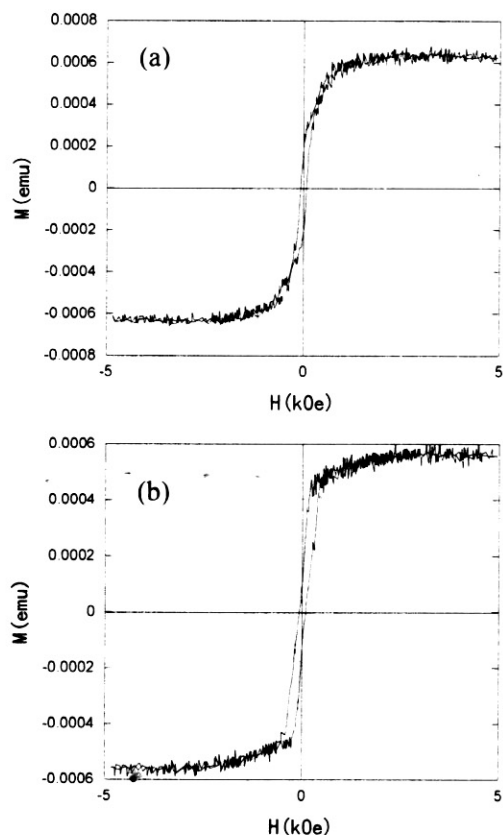


Fig. 8 (a) AFM image and (b) MFM image obtained by using a low-moment tip.

of more than 100 nm have strong perpendicular anisotropy and that the feature of low remanence is not changed, suggesting that the anisotropic behavior originates in the shape anisotropy.

We also measured the hysteresis loops of Co dot arrays with the same shapes and configurations.  $H_c$  and  $M_r/M_s$  were 50 Oe and 0.44, respectively, for the in-plane magnetic field, and 130 Oe and 0.81, respectively, for the perpendicular field. We consider that the Co dot arrays have a single domain structure with a perpendicular magnetization in the remanence state.



**Fig.9** Hysteresis loops of circular dots with a radius of 100 nm. (a) Parallel direction and (b) perpendicular direction to the surface.

### 3.5 Nonlinear magneto-optical studies

The nonlinear magneto-optical effect is known to provide a large amount of information on the magnetism of surfaces and interfaces.<sup>9)</sup> It also provides information on crystallographic and magnetic symmetry, as evidenced by our study on the magnetization-induced second harmonic generation (MSHG) in Fe/Au artificial superlattices, in which we found four-fold rotation symmetry that reflects the symmetry of the MgO substrate.<sup>10)</sup> However, MSHG measurement of dot array structures has proved difficult, because of strong scattering by the structured surfaces.

Since our nanostructures have a flat surface, we can use them as samples for nonlinear magneto-optical studies. Using the square and rectangular dot-array structures prepared in this study, we recently observed strong MSHG signals with four-fold and two-fold rotational symmetry, respectively, corresponding to the artificial symmetry of the dot-arrays. Details of the study will appear in later publication.<sup>11)</sup>

## 4 Summary

Permalloy dot arrays as small as 100 nm in areal dimension and more than 100 nm in height were successfully fabricated using the damascene technique. The magnetic properties of three kinds of samples were

investigated. Square dots with dimensions of  $1\ \mu\text{m} \times 1\ \mu\text{m}$  in area and 100 nm in height showed  $90^\circ$ -domain wall structures, while rectangular dots with a area of  $300\ \text{nm} \times 100\ \text{nm}$  and a height of 100 nm had a sort of three-dimensional vortex structure. The perpendicular anisotropy became stronger in circular dots with a diameter of 100 nm and a depth of 100 nm. These results indicate that the direction of the easy axis varies from parallel to perpendicular as the dot size decreases and the aspect ratio increases. It was also shown that accurate MFM measurement in small magnetic dot-structures of sub-micrometer size require a reduction of magnetic field effects from the magnetic tips. Use of low-moment tips in a vacuum environment was proved helpful to obtaining accurate magnetic images.

### Acknowledgements

The authors are very grateful to Dr. Yamaoka of Seiko Instruments Inc. for his help in MFM measurements with a low-moment tip. This work has been carried out under the 21st-century COE program of TUAT on "Future Nano Materials."

### References

- 1) S. Y. Chou, M. S. Wei, P. R. Krauss and P. B. Fischer, *J. Appl. Phys.*, **76**, 6673 (1994).
- 2) C. A. Ross, S. Haratani, F. J. Castaño, Y. Hao, M. Hwang, Shima, J. Y. Cheg, B. Vögeli, M. Farhoud, M. Walsh, and H. I. Smith, *J. Appl. Phys.* **91**, 6848 (2002).
- 3) X. Zhu, P. Grütter, V. Metlushko, and B. Ilic, *Phys. Rev.* **B66**, 024423 (2002).
- 4) J. Lohau, A. Moser, C. T. Rettner, M. E. Best, and B. D. Terris, *Appl. Phys. Lett.*, **78**, 990 (2001).
- 5) R. D. Gomez, T. V. Luu, A. O. Pak, K. J. Kirk, and J. N. Chapman, *J. Appl. Phys.*, **85**, 6163 (1999).
- 6) T. Aoyama, S. Okawa, K. Hattori, H. Hatate, Y. Wada, T. Kagotani, K. Uchiyama, H. Nishio and I. Sato, Proceedings of the Technical Meeting on Magnetism, IEEJ, MAG-00-323 (2000).
- 7) J. M. Garcia, A. Thiaville, J. Miltat, K. J. Kirk, J. N. Chapman, and F. Alouges, *Appl. Phys. Lett.*, **79**, 656 (2001).
- 8) T. Yamaoka, K. Watanabe, Y. Shirakawabe, and K. Chinone, *J. Magn. Soc. Jpn.*, **27**, 429 (2003).
- 9) K. H. Bennemann(ed.), *Nonlinear Optics in Metals*, (Clarendon Press, Oxford, 1998).
- 10) K. Sato, A. Kodama, M. Miyamoto, A.V. Petukhov, K. Takashi, S. Mitani, H. Fujimori, A. Kirilyuk, and Th. Rasing, *Phys. Rev.* **B64**, 184427 (2001).
- 11) S. Shimizu, T. Matsumoto, T. Ishibashi, A. Koukitu, and K. Sato, to appear in Extended Abstracts of the 26th Annual Conference on Magnetism in Japan (Osaka, 2003).

Received May 12, 2003; Accepted July 16, 2003.